International Journal of Astrobiology 8 (3): 147–159 (2009) Printed in the United Kingdom
doi:10.1017/S1473550409990073

The Sun, geomagnetic polarity transitions, and possible biospheric effects: review and illustrating model

Karl-Heinz Glassmeier[1,2], Otto Richter[3], Joachim Vogt[4], Petra Möbus[5] and Antje Schwalb[6]

[1]*Institut für Geophysik und extraterrestrische Physik, Technische Universität Braunschweig, Mendelssohnstrasse 3, D-38106 Braunschweig, Germany*
[2]*Max-Planck-Institut für Sonnensystemforschung, Max-Planck-Strasse 2, D-37191 Katlenburg-Lindau, Germany*
e-mail: kh.glassmeier@tu-bs.de
[3]*Institut für Geoökologie, Technische Universität Braunschweig, Langer Kamp 19c, D-38106 Braunschweig, Germany*
[4]*School of Engineering and Science, Jacobs University Bremen, Campus Ring 1, D-28759 Bremen*
[5]*Johann Heinrich von Thünen Institut, Bundesallee 50, D-38116 Braunschweig, Germany*
[6]*Institut für Umweltgeologie, Technische Universität Braunschweig, Pockelsstrasse 3, D-38106 Braunschweig, Germany*

Abstract: The Earth is embedded in the solar wind, this ever-streaming extremely tenuous ionized gas emanating from the Sun. It is the geomagnetic field which inhibits the solar wind plasma to directly impinge upon the terrestrial atmosphere. It is also the geomagnetic field which moderates and controls the entry of energetic particles of cosmic and solar origin into the atmosphere. During geomagnetic polarity transitions the terrestrial magnetic field decays down to about 10% of its current value. Also, the magnetic field topology changes from a dipole dominated structure to a multipole dominated topology. What happens to the Earth system during such a polarity transition, that is, during episodes of a weak transition field? Which modifications of the configuration of the terrestrial magnetosphere can be expected? Is there any influence on the atmosphere from the intensified particle bombardment? What are the possible effects on the biosphere? Is a polarity transition another example of a cosmic cataclysm? A review is provided on the current understanding of the problem. A first, illustrating model is also discussed to outline the complexity of any biospheric reaction on polarity transitions.

Received 19 March 2009, accepted 27 May 2009, first published online 2 July 2009

Key words: energetic particles, geomagnetic field, ozone hole, ozonosphere, paleomagnetosphere, phytoplankton, polarity transition, solar wind, Sun, UV-B stress.

1 Geomagnetic variations and the paleomagnetosphere

For about 3.2 billion years planet Earth has had a global magnetic field (e.g. Tarduno *et al*. (2007)). This geomagnetic field is not at all stable, but exhibits major temporal changes, such as geomagnetic variations. Currently the magnetic dipole moment is showing a dramatic decrease, with about a 10% decay since 1840 or a 0.5% decay per decade (Fig. 1). If the current decrease continues the geomagnetic dipole field will vanish in about 2000 years.

However, the most dramatic changes in the geomagnetic field are polarity transitions, which are events during which the dipole component of the geomagnetic field changes its polarity. Convincing evidence for such changes are found by paleomagnetic studies (e.g. Soffel (1991), Merrill & McFadden (1999)). Polarity transitions are non-periodic events affecting the geodynamo. Over the last 5 million years paleomagnetic studies have revealed about 20 transitions, which implies a transition time scale of the order of 250 000 years. As the last one, the Matuyama–Brunhes reversal, occurred 780 000 years ago it is tempting to expect a further transition geologically soon.

The duration of a polarity transition is of the order of 10 000 years (Fig. 2), a time span short on geological time scales, but long enough for possible effects on the biosphere. Paleomagnetic studies demonstrate (e.g. Leonhardt & Fabian (2007)) that a reversal can be characterized by an increase of the non-dipolar contribution to the surface magnetic field followed by a decrease of the dipolar contribution. During a transition the surface magnetic field strength of the Earth decays to about 10% or less of its present value. This does not imply that the geodynamo ceases to operate. Although the dipole moment significantly decays, the dynamo still generates magnetic field energy efficiently in higher order multipole moments such as the quadrupole or octupole. As these non-dipolar field contributions are spatially faster decaying than the dipole contribution, the magnetic field magnitude is effectively lowered at the Earth surface. A polarity transition is thus characterized by a decaying dipole moment,

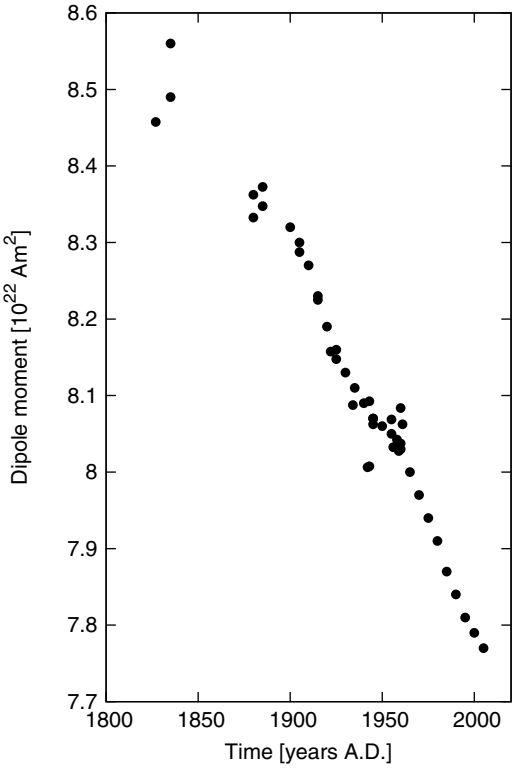

Fig. 1. Decay of the dipole moment of the geomagnetic field during the last 200 years (from Glassmeier *et al.* (2009)).

a weakened surface field strength and a more complex field topology.

This led to the conjecture that the currently observed decay of the dipole moment indicates a polarity transition occurring soon. This conjecture needs to be considered with care as paleomagnetic studies also reveal that about 12 000 years ago the dipole moment was about 50 % larger than today's value (e.g. Korte & Constable (2006)). This implies the possibility that we are just facing a situation of normalizing dipole moment. Further arguments against a transition occurring soon are, for example, that the present field strength is nearly twice the long-term average field strength and that the present field is approximately equal to the field during the mid-Cretaceous when it did not reverse for about 40 million years (Selkin & Tauxe 2000). Nevertheless, a polarity transition, if it happens, is a major change to the Earth system and needs further attention as a process with possible impact on the evolution of life on our planet.

Numerous attempts have been reported to find any correlation between geomagnetic polarity transitions and faunal extinctions (e.g. Uffen (1963), Black (1967), Watkins & Goodell (1967), Hays (1971), Raup (1985)). None of these can be regarded as conclusive. Of particular interest is the detailed study by Hays (1971), who studied a larger number of piston cores from high and low geographic latitude marine locations indicating that during the last 2.5 million years several species of radiolaria became extinct (Fig. 3). Some of these species, such as *Clathrocyclas bicornis* or *Pterocanum prismaticum*, disappeared in close proximity to magnetic

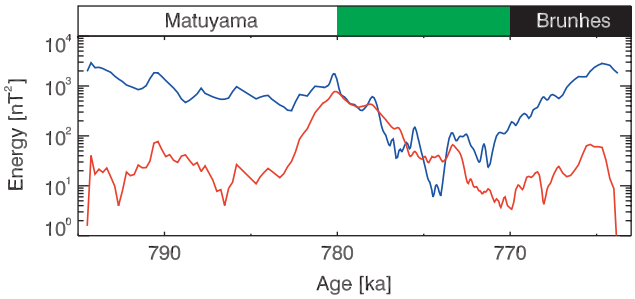

Fig. 2. Temporal magnetic energy variation of dipolar (blue line) and non-dipolar (red line) field components at the Earth's surface during the Matuyama–Brunhes polarity transition. The Mauersberger coefficient has been used as a measure of the magnetic field energy (modified after Fabian & Leonhardt (2009)).

polarity transitions recorded in the sediment. Other species, for example *Stylatractus universus* and *Druppatractus acquilonius*, did survive several reversals. The evidence, however, is strongly suggestive that polarity transitions either directly or indirectly exert a selective force in some species and evidence is mounting that Earth's magnetic field may play an important role in the development of life on planet Earth. However, for a critical discussion of the problems associated with correlation studies between geomagnetic and sedimentary data reference is made to Mann (1972), Hays (1972) and Plotnick (1980).

The natural question arising then is what processes could cause such a relation between polarity transitions and the Earth system. The Sun and its activity plays an important role in answering this question. On the one hand, the Sun continuously emits the solar wind, a hot magnetized plasma streaming into interplanetary space with velocities of several hundred kilometers per second. On the other hand, the Sun is also a significant source of energetic particles. Numerous reports about solar energetic particle (SEP) events exist and show that planet Earth is regularly bombarded by protons in the MeV to several hundred MeV energy range (Mewaldt 2006).

An immediate consequence of the geomagnetic field is its ability to prevent solar wind particles from impeding the atmosphere and Earth surface. A magnetosphere (e.g. Kallenrode (2004)) is formed around the Earth with the magnetopause separating the hot solar wind plasma from the magnetospheric plasma (see Fig. 4). On the dayside the geomagnetic field is compressed by the solar wind; on the nightside the magnetic field lines are stretched out to form a long magnetotail. The regime thus formed, the magnetosphere, is separated from the solar wind plasma by the magnetopause boundary. The sub-solar stand-off distance of this magnetopause, R_{MP}, is related to the solar wind dynamic pressure $p_{dyn} = 1/2\rho v^2$ and the equatorial geomagnetic field strength B_0 via

$$R_{MP} = \sqrt[6]{\frac{4\,B_0^2}{\mu_0 \cdot p_{dyn}}}, \qquad (1)$$

https://doi.org/10.1017/S1473550409990073 Published online by Cambridge University Press

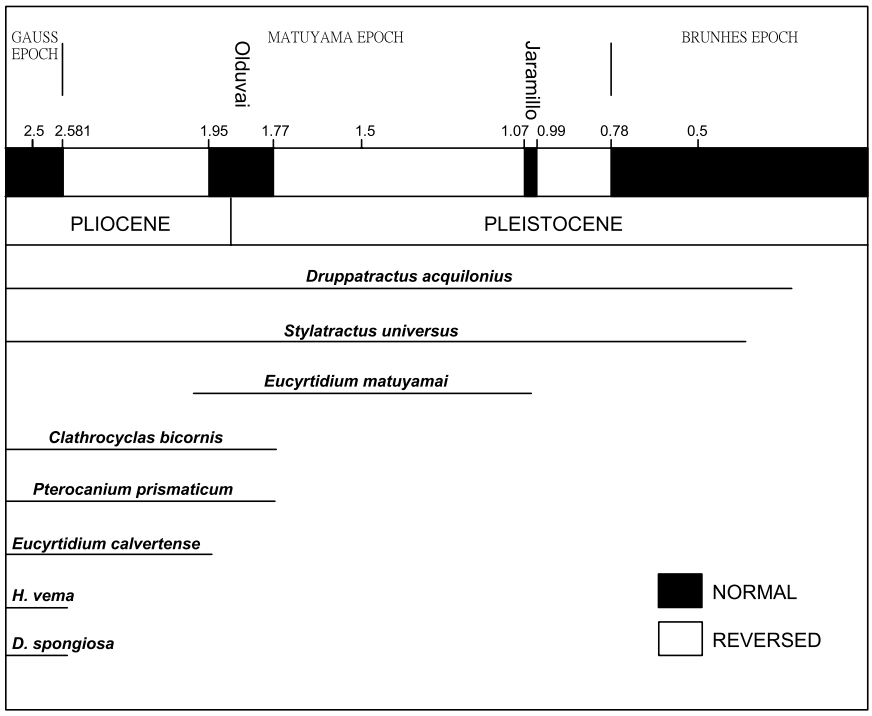

Fig. 3. Radiolaria extinction associated with paleomagnetic epochs and events (after Hays (1971)).

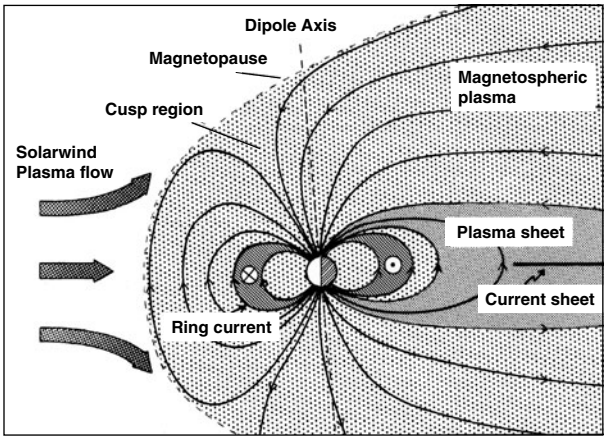

Fig. 4. The terrestrial magnetosphere (from Glassmeier *et al.* (2009)).

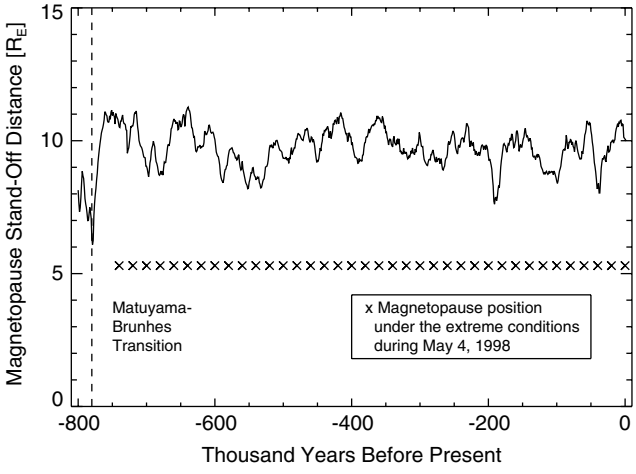

Fig. 5. The mean magnetopause stand-off distance during the last 800 00 years, based on the SINT-800 paleomagnetic intensity data Guyodo & Valet (1999). The vertical dashed line indicates the Matuyama–Brunhes transition. The horizontal crossed line gives the position of the magnetopause during the extreme solar wind conditions of 4 May 1998 (after Glassmeier *et al.* (2004)).

where ρ and v denote the solar wind mass density and velocity, respectively. For typical contemporary solar wind conditions a stand-off distance of $R_{MP} = 65\,000$ km results.

What happens to the magnetopause distance during a polarity transition when the surface magnetic field significantly decreases? Siscoe & Chen (1975) were amongst the first to investigate this problem. As the stand-off distance R_{MP} scales with the cubic root of the equatorial magnetic field strength, $R_{MP} \propto \sqrt[3]{B_0}$, a decreasing dipole moment implies a shrinking of the magnetosphere.

Can it vanish at all? Based on paleomagnetic field intensities compiled by Guyodo & Valet (1999), Fig. 5 displays the evolution of the mean magnetopause stand-off distance during the last 800 000 years (see Glassmeier *et al.* (2004) for further details). On average the magnetopause was never closer than 57 000 km to the Earth's surface. Only during the last polarity transition did the interface between the solar wind and the magnetosphere move down to about 38 000 km, that is, a geostationary spacecraft would have been immersed in the solar wind. Only for extreme solar wind conditions as observed, for example, on 4 May 1998 with solar wind velocities of 800 km s^{-1} did the magnetopause move downward to heights of 32 000 km. If such extreme conditions

https://doi.org/10.1017/S1473550409990073 Published online by Cambridge University Press

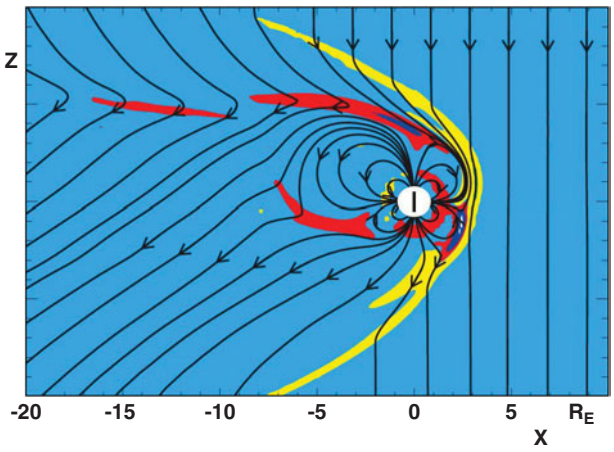

Fig. 6. Magnetohydrodynamic simulation of a quadrupolar magnetosphere in the $x-z$ plane, i.e. the plane containing the Earth rotation axis. The IMF direction is perpendicular to the solar wind flow. Black lines indicate magnetic field lines. Electric current flow is represented by filled coloured contours; currents into the plane are indicated as red, currents out of the plane are indicated as yellow (after Vogt *et al.* (2004)).

occurred also during a polarity transition the magnetopause distance would move down to about 20 000 km. This clearly indicates that, most probably, the magnetosphere also exists during a typical polarity transition with the magnetopause never reaching a height where it can directly influence the terrestrial atmosphere. The study by Glassmeier *et al.* (2004) also indicates that the solar wind dynamic pressure is the more important driver for positional changes of the magnetopause as this pressure exhibits a much larger variability than the geomagnetic field.

These considerations show that the magnetosphere will shrink if the geomagnetic field strength varies as observed during a polarity transition. But what about the topology of the magnetosphere, does it depend on the topology of the geomagnetic field? As mentioned above (cf. Fig. 2) non-dipolar field components can dominate the geomagnetic field during a polarity transition. Vogt & Glassmeier (2000), Vogt *et al.* (2004), Zieger *et al.* (2004) and Zieger *et al.* (2006) have extensively studied this problem. As an example of their results Fig. 6 displays the structure of a quadrupole magnetosphere, that is, a magnetosphere whose internal magnetic field is dominated by a quadrupolar geomagnetic field. The situation displayed is that of an equator-on configuration with the quadrupole aligned with the Earth rotation axis. The interplanetary magnetic field (IMF) is assumed to be perpendicular to the solar wind flow. The resulting field structure is complex. The magnetopause is easily identified by the electric currents flowing out of the $x-z$ plane, i.e. the plane perpendicular to the ecliptic. Other current systems are emerging as well and help to shape the complex magnetotail structure. The simulations also indicate that paleomagnetospheric dynamics in non-dipolar configurations should be very persistent rather than being strongly dependent on the orientation of the interplanetary magnetic field, which controls the dynamics of the present day magnetosphere.

Worth noting are also the multiple cusp regions, which are regions where energetic particles can easily enter the magnetosphere proper. In the current dipole-field-dominated terrestrial magnetosphere the northern and southern cusp regions are those regions where the aurora borealis and the aurora australis, respectively, are observed. The possible appearance of multiple cusp regions and associated auroral displays at mid and low latitudes has already been noted by Siscoe & Crooker (1976). These authors also speculate about a possible cultural effect on early human societies. However, as the magnetosphere always exists no direct catastrophic effect during a polarity transition is expected based on the above-referenced studies.

2 Energetic particles and the atmosphere

The paleomagnetosphere exists under all known conditions and is a shield for planet Earth against the solar wind plasma. But is it also a shield against very energetic particles of solar and cosmic origin? Studies by, for example, McHargue *et al.* (2000) and Baumgartner *et al.* (1998) demonstrate a clear correlation between secular variations of the geomagnetic field intensity and enhanced cosmic-ray production of ^{10}Be or ^{36}Cl. These studies indicate that the geomagnetic field is at least strongly moderating the access of energetic particles into the magnetosphere and atmosphere. A possible link between the geodynamo and the biosphere is via the effect of these energetic particles on the atmosphere.

For example, Tinsley & Deen (1991) and Svensmark *et al.* (2007) discuss a connection via electro-freezing of supercooled water in the troposphere. For a more detailed review on this process and its possible influence on the Earth system reference is made to Svensmark (2007).

Here we concentrate on another possible link – NO_X and HO_X increases in the middle atmosphere induced by energetic particle bombardment, and the subsequent vertical transport of these molecules down to the stratosphere where a clear decrease of the ozone column density should result. This in turn implies a significantly increased level of UV-B radiation with possible effects on the biosphere. This chain of interactions is well established by recent observations of very large particle events from solar eruptions, so-called solar proton events (SPEs) and their effects on the atmosphere (e.g. Crutzen *et al.* (1975) and Jackman *et al.* (2001)).

During a normal SPE these atmospheric effects are minor, yet detectable. A long-duration decrease of the stratospheric ozone, however, and an increase of the UV-B is not expected due to such normal SPEs. The consequences of a tropospheric UV-B increase are the topic of many studies (e.g. Cockell & Blaustein (2001)). For many decades the total ozone column has been measured continuously at different locations on the Earth and in orbit. The results indicate a current latitude-dependent decrease of the stratospheric ozone with major effects observed in the polar region, that is, in the so-called ozone hole (e.g. Solomon (1988) and

https://doi.org/10.1017/S1473550409990073 Published online by Cambridge University Press

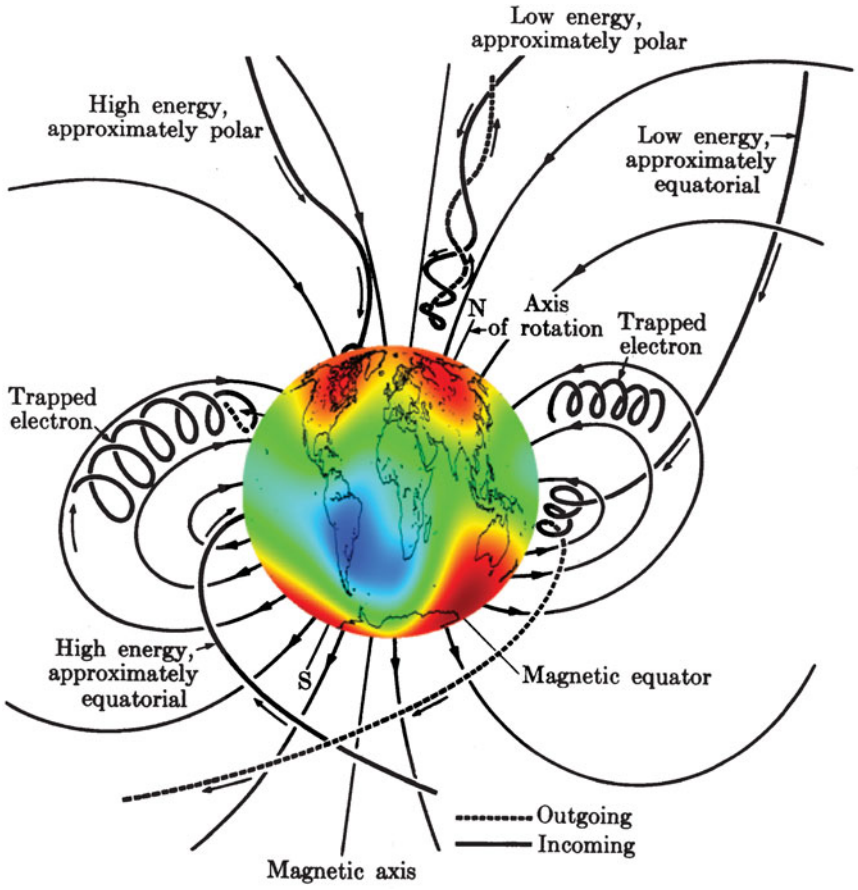

Fig. 7. Energetic particles and the geomagnetic field. Red areas denote the geomagnetic pole regions with their large field strength; the blue regime is the south Atlantic anomaly (from Glassmeier *et al.* (2009)).

Staehelin *et al.* (2001)). A decrease in the stratospheric ozone is expected to be accompanied by an increase in tropospheric UV radiation as the stratospheric ozone constitutes a filter against harmful UV-B radiation. Thus, a reduction of total ozone causes an increase in the terrestrial erythemal irradiation dose (e.g. Casale *et al.* (2000)).

A significant increase of UV-B radiation at the surface, caused by a major decrease of stratospheric ozone due to very energetic ionized particles accessing the middle atmosphere, is a viable process via which the biosphere can suffer. The question to be posed is in which way the geomagnetic field is controlling the access of energetic particles to the atmosphere. Figure 7 schematically indicates the fate of energetic particles in the geomagnetic field. In a dipole field dominated structure low-energy particles are reflected in polar regions or are trapped in the geomagnetic field unless their pitch angle is very small. Higher energy particles can penetrate much deeper into the polar regions and reach the middle atmosphere. Whether a particle is a low- or high-energy particle is a relative classification and depends on the strength of the geomagnetic field. The gyroradius

$$r_G = \frac{m\ v_\perp}{|q|\ B} \qquad (2)$$

is a useful measure in this respect; m, q, B and $v_\perp$ denote mass and charge of the particle, the magnetic field strength and the particle's transverse velocity, respectively. A small (large) gyroradius implies that the particle is (not) much influenced by the magnetic field. Thus, during a polarity transition with its small surface magnetic field strength low-energy particles have a much larger gyroradius and a better access to the atmosphere.

Another very useful measure to describe the impact of energetic particles on the atmosphere is the so-called cut-off latitude, which defines the geomagnetic latitude a particle with given energy can reach (e.g. Smart *et al.* (2000)). The concept of the cut-off latitude is, however, only useful for almost dipolar geomagnetic field topologies. During a polarity transition with its strong multi-polar contributions the cut-off latitude concept is less useful. Stadelmann (2004), Vogt *et al.* (2007) and Stadelmann *et al.* (2009) introduced and used the concept of an impact area to describe the influence of energetic particles on the atmosphere. The impact area is defined as the surface area reached by particles of a given energy normalized to the total surface area of Earth.

To determine this impact area a particle tracing scheme was combined with a potential field model of the magnetospheric magnetic field. Following Voigt (1981) the dayside

https://doi.org/10.1017/S1473550409990073 Published online by Cambridge University Press

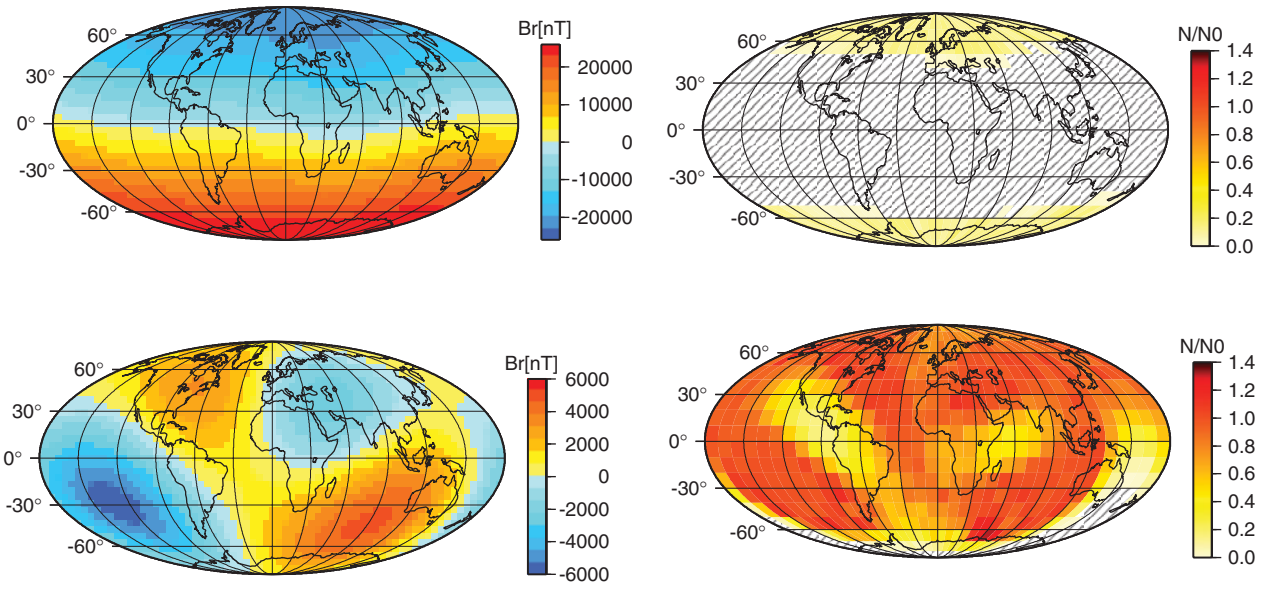

Fig. 8. The spatial distribution of the radial component of the Earth magnetic field (left) and regions on the globe that become accessible to 256 MeV protons (right) before and during a simulated polarity reversal. Top: 15 000 years before the reversal. Bottom: At the time of the reversal (after Stadelmann (2004)).

and nightside of the magnetopause are assumed to be spherical and cylindrical, respectively. The normal component of the magnetic field at the magnetopause is used as a parameter to model different levels of magnetospheric activity and the internal field can be chosen as an arbitrary combination of dipolar and quadrupolar contributions (Stadelmann 2004; Stadelmann *et al.* 2009). The model is sufficiently flexible to construct various paleomagnetospheric situations.

As an example, Fig. 8 displays those regions of the Earth's surface reachable by 250 MeV particles before and during a polarity transition. The dynamo generated magnetic field configurations are from the numerical simulation of Glatzmaier & Roberts (1995), the resulting magnetospheric configuration determined with the potential field model outlined. For the pre-reversal situation, that is, the current magnetic field, only the polar regions can be reached by energetic particles. The cut-off latitude is at about 60°. During the reversal, however, most of the Earth's atmosphere is impacted by energetic particles. The impact area amounts to about 95%.

If most of the Earth's surface suffers from the impact of energetic particles during a polarity transition, then the question emerges concerning which atmospheric effects are likely to occur. Based on the processes suggested by, for example, Crutzen *et al.* (1975), Sinnhuber *et al.* (2003) and Winkler *et al.* (2008) studied this problem in more detail assuming that the impacting energetic particles are solar energetic protons. A global two-dimensional photochemical and transport model of the stratosphere and mesosphere is used to investigate the situation. Atmospheric ionization is calculated based on measured proton fluxes with the NO_X and HO_X production rates parameterized such that good agreement between modelled and actually measured NO_X production and ozone loss during a number of SPEs of recent years is achieved. The model furthermore allows one to determine the loss of total ozone in the atmosphere and the surface UV-B radiation. For details reference is made to Sinnhuber *et al.* (2003), Winkler *et al.* (2008) and Vogt *et al.* (2009).

A rather simple worst-case scenario was modelled assuming that during a polarity transition the geomagnetic field vanishes completely. This implies that energetic particles have maximum access to the atmosphere. This scenario allows one to determine what influence SPEs have on the atmosphere without being modified by any geomagnetic field. A series of three SPEs with proton fluxes and ionization rates obtained from measurements during the October 1989 solar event (e.g. Reid *et al.* (1991)) were modelled. The resulting change of total ozone is shown in Fig. 9. The total ozone loss reaches more than 40% (10%) in the northern (southern) hemisphere. The northern hemisphere loss is significantly larger than for the man-made polar ozone hole. Also, contrary to the man-made ozone hole the SPE-induced paleo-ozone hole is not restricted to polar spring, but continues into the following years.

The observed interhemispheric difference is not due to any asymmetry in the proton precipitation, but a result of meridional circulation. The NO_X molecules are first produced in the middle atmosphere, well above the ozone layer. To effect the ozonosphere the NO_X particles have to be transported down to the stratosphere. This happens only during polar winter, when large-scale downward transport of atmospheric gas masses occurs. In regions other than the polar

https://doi.org/10.1017/S1473550409990073 Published online by Cambridge University Press

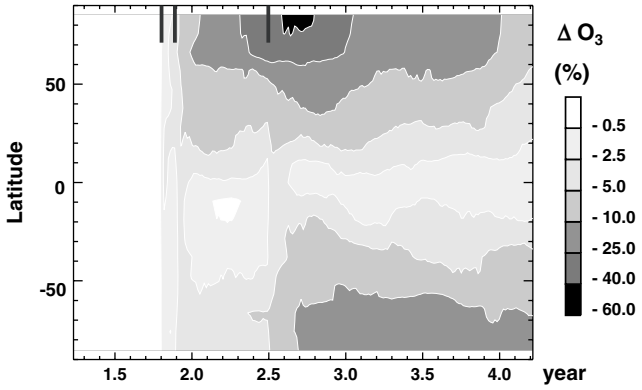

Fig. 9. Modelled change of the total ozone as a function of latitude and time. The influence of three consecutive SPEs (onsets indicated by vertical bars) has been modelled assuming an Earth without any global magnetic field (after Sinnhuber *et al.* (2003)).

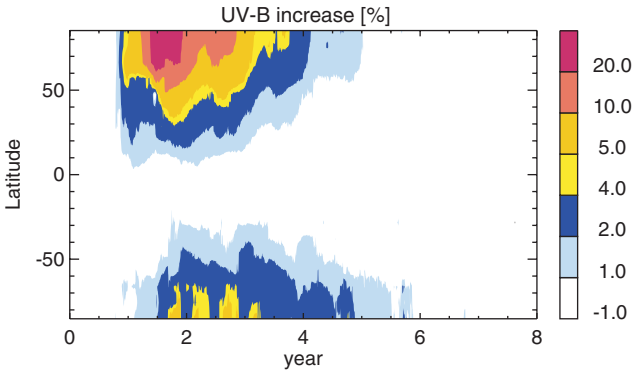

Fig. 10. Modelled change of erythemal weighted surface UV-B flux for an average geomagnetic field configuration during a polarity transition and assuming SPE activity as in Fig. 9 (after Winkler *et al.* (2008)).

regions, NO_X molecules remain in the middle atmospheric layers and decrease in density due to solar radiation. Thus the polar regions are most favourable for ozone depletion during SPEs.

For a different scenario with non-vanishing geomagnetic field the modelled change of the surface UV-B is displayed in Fig. 10. The geomagnetic field is assumed to be a combined axisymmetric dipole–quadrupole field, which according to Constable & Parker (1988) is a reasonable average reversal situation. The moments are chosen such that both multipoles contribute equally to the surface magnetic field strength at the northern pole and are oppositely directed at the southern pole. The field strength is assumed to be 10 % of the present day value. Different polar caps result for this geomagnetic field situation: the northern polar cap has a width of about 60°, while the southern one a width of 30°. Particle precipitation mainly occurs in these polar cap regions. For further details reference is made to Vogt *et al.* (2007) and Winkler *et al.* (2008).

In model years 1–4 a significant increase of the surface UV-B flux, that is, radiation in the wavelength range 280–315 nm, is observed. The increase is largest in polar latitudes, especially in the northern hemisphere. However, the southern hemisphere also suffers from a clear increase in radiation. The maximum increase amounts to about 20 %, a value comparable to the altitude increase per 1000 m in an Alpine environment (e.g. Gröebner *et al.* (2000)) and three to five times as large as the annually averaged surface UV-B increase caused by the anthropogenically generated ozone hole (e.g. Madronich *et al.* (1998)).

The Winkler *et al.* (2008) model calculations also indicate a significant change of the atmospheric temperature. During the SPEs a cooling of the middle atmosphere is observed associated with a warming below the 50–70 km altitude range. Another region of cooling occurs at an altitude of around 20 km. However, no significant temperature effect is modelled for the troposphere. The studies by Sinnhuber *et al.* (2003), Vogt *et al.* (2007) and Winkler *et al.* (2008) thus suggest that a major effect of energetic particle precipitation into the paleomagnetosphere is the build-up of a natural ozone hole associated with significantly increased UV-B radiation levels in polar regions. Although the UV-B level recovers to background levels a few years after the SPEs possible impacts on the biosphere cannot be excluded.

3 Effects on aquatic ecosystems: an illustration

The role of ultraviolet radiation has already been discussed by Marshall (1928) when speculating about factors controlling extinction. Whether extinctions are caused or influenced by geomagnetic polarity transitions has been the subject of numerous studies, but the results are still very unclear and contradictorily. Whether a polarity transition constitutes a global catastrophe to planet Earth is not at all clear. Sediments are the best archive to search for indications of such global catastrophes and their relation to geomagnetic field changes (e.g. Hays (1971)).

As the studies by Sinnhuber *et al.* (2003), Vogt *et al.* (2007) and Winkler *et al.* (2008) demonstrate the possibility of generating a natural ozone hole during reversals, it is necessary to further study the stress of enhanced UV-B radiation on ecosystems. The UV-B radiation effects of the modelled ozone hole are dominant in polar regions. Thus, as a first step to understand any ecological effect of the hypothesized UV-B increase, it is interesting to have a look into the effects on aquatic ecosystems. Numerous studies on this problem have been published. In the following, as an illustrative example, we present a conceptual model allowing one to infer the reaction of phytoplankton to UV-B stress (Fig. 11). For a more detailed review reference is made to Häder (2001). Here we are mainly interested in outlining the complexities in the following process chain: (a) polarity transition; (b) SPE; (c) middle atmospheric NO_X production; (d) decreasing ozone density; (e) increased UV-B level; and (f) biospheric effects. Understanding this process chain in more detail is necessary to better understand any statistical analysis of paleomagnetic field data and biospheric signals such as extinctions of flora and fauna.

https://doi.org/10.1017/S1473550409990073 Published online by Cambridge University Press

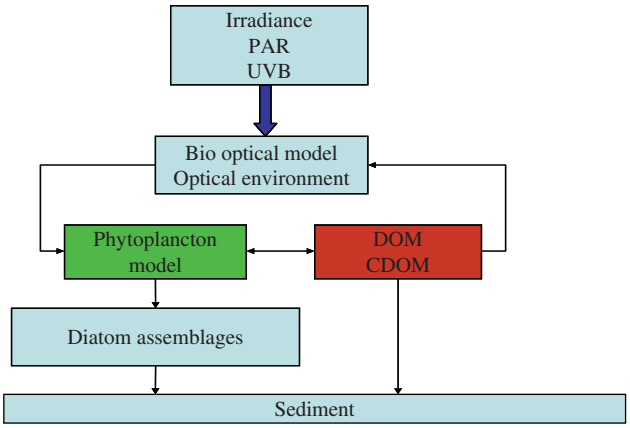

Fig. 11. Conceptual model of the interaction of irradiation and the benthic system. The optical environment is determined by plankton density, dissolved organic matter (DOM) and chromophoric dissolved organic matter (CDOM). The release of CDOM provides protection against UV-B irradiation.

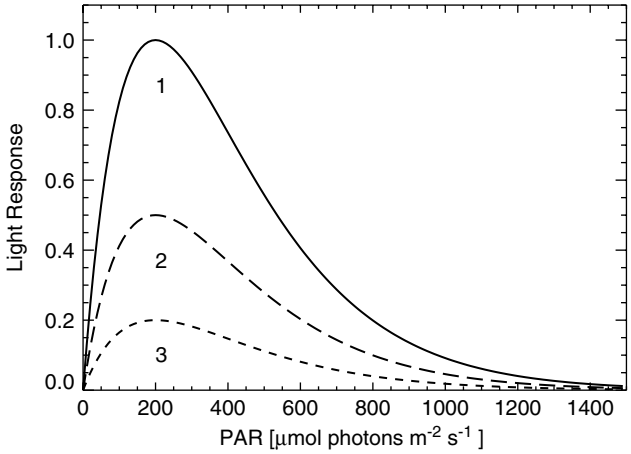

Fig. 12. Normalized response curve (Eqn 5) of the rate of photosynthesis in phytoplankton dependent on the PAR for different UV-B levels (1: no UV-B, 2: threshold level, 3: above threshold level).

Here, we provide a model which involves the interaction of phytoplankton dynamics with the optical environment of the water column, which allows us to gain an insight into the reaction of an aquatic model ecosystem to UV-B stress. The conceptual model is shown in Fig. 11. We consider a phytoplankton population in a water column. The growth rate is dependent on the irradiation in the photosynthetically active radiation (PAR) wavelength range. Growth is inhibited by UV-B radiation surpassing an intensity threshold. The optical environment is influenced by phytoplankton density, dissolved and particulate organic matter, and by chromophoric dissolved organic matter with the capability of absorption of UV-B (e.g. Kuwahara *et al.* (2000)). There is some evidence that plankton species exist that are capable of releasing chromophoric substances (e.g. Häder *et al.* (2007), Steinberg *et al.* (2004) and Morrison & Nelson (2004)) thus providing UV-B photo protection. Our model allows for negative phototaxis, i.e. the plankton is able to migrate to a zone of diminished radiation intensity avoiding the layers near the surface in daytime. Our interest is in studying the population dynamics of plankton and the role of CDOM under elevated UV-B levels as they can occur during polarity transitions. We simulate the polarity transition triggered UV-B increase as an outbreak of UV-B intensity above the threshold and study the effects of this outbreak on the phytoplankton population and CDOM production. Due to gravitational settling it is to be expected that CDOM accumulates in the sediment, where it could be detected as a proxy for UV-B increases.

The temporal change of the density of the phytoplankton population B of our one-dimensional model is described by the following equation:

$$\frac{\partial B}{\partial t} = P(I_{PAR}, I_{UVB}) \cdot B \cdot \left(1 - \frac{B}{C_B}\right) + \frac{\partial}{\partial z}\left(D_B \frac{\partial}{\partial z} B - B\, v_Z\right) - \beta \frac{H \cdot B}{B + K_S} - \mu B. \tag{3}$$

Here $P(I_{PAR}, I_{UVB})$ denotes the rate of photosynthesis, PAR is the photosynthetically active radiation, C_B the capacity of the phytoplankton population, D_B a diffusion coefficient of the phytoplankton, v_Z the vertical component of active plankton motion and gravitational settling, H the herbivore density, β the maximum consumption rate per herbivore, K_S a saturation constant and μ the phytoplankton mortality rate. Here, we do not consider the whole nutritional chain, but only consider the primary producer. In the subsequent model calculations consumption by herbivores was therefore omitted. For further details see Klausmeier & Lichman (2001) and Chattopadhyay & Sarkar (2003).

The first term of this equation describes the phytoplankton growth, the second is a dispersal term and the third describes the mortality due to predation and intrinsic mortality. Growth is limited by the retardation factor in analogy to logistic growth with the capacity parameter C_B reflecting nutritional constraints.

The dispersal term takes into account random movement in form of diffusion and active movement driven by the deviation of light intensity from an optimal value (negative phototaxis). So in the night the plankton moves against the gravitational field (negative gravitaxis) and in the daytime the plankton moves into the region of optimal PAR light intensity. However, reaching an optimal PAR level can be of disadvantage if this optimal level is at a depth of strong UV-B intensity. These effects are described by the first term of the equation

$$v_Z = \alpha \cdot (I_{PAR}(z, t) - I_{OPT}) - v_g, \tag{4}$$

where α is a scaling factor, z the vertical position and I_{OPT} the optimal flux density for PAR; v_g denotes gravitational settling.

In contrast to land plants, the light response of many plankton species is characterized by a unimodal optimum

https://doi.org/10.1017/S1473550409990073 Published online by Cambridge University Press

Table 1. *Model parameters**

Parameter	Meaning	Value
I_{PAR}	photosynthetically active radiation at the upper boundary of the water column [μmol photons $m^{-2} s^{-1}$]	1400
I_{opt}	optimal radiation density [μmol photons $m^{-2} s^{-1}$]	200
κ_B	background attenuation coefficient for PAR [m^{-1}]	0.35
κ_P	attenuation coefficient for PAR due to algal biomass [m^{-1}/(cell density)]	0.6
σ_B	background attenuation coefficient for UV-B [m^{-1}]	0.3
σ_P	attenuation coefficient for UV-B due to CDOM [m^{-1}/(mol CDOM)]	0.6
C_B	capacity of phytoplankton population (maximum density) [10^5 cells ml^{-1}]	1
p_{max}	maximum growth rate [h^{-1}]	0.4
μ	loss rate [h^{-1}]	0.01
D_B	eddy diffusion coefficient for plankton movement [$m^2 h^{-1}$]	0.8
D_{CDOM}	diffusion coefficient for CDOM [$m^2 h^{-1}$]	0.8
α	parameter for active velocity of plankton [m h^{-1} μmol^{-1} photons $m^{-2} s^{-1}$]	0.0015
v_g	velocity of gravitational settling [m h^{-1}]	0.008
γ	kinetic constant for production of CDOM under enhanced UV-B stress [h^{-1}]	1.8
K_{tr}	UV-B threshold for inhibition of photosynthesis [μmol photons $m^{-2} s^{-1}$]	70
m	form factor for the steepness of threshold	2

* Parameter values partly from Klausmeier & Lichman (2001).

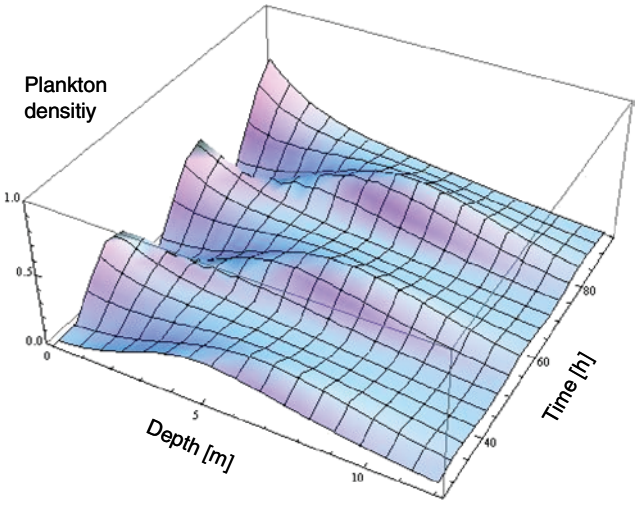

Fig. 13. Time course of plankton density profiles. This simulation shows the effect of phototaxis. The plankton migrates to the zone of optimal radiation intensity avoiding the layers near the surface in the daytime. At night the density maximizes.

function (Eilers & Peeters 1988; Steele 1962). In the following model, the rate of photosynthesis is described by a unimodal response function. Photosynthesis is inhibited by UV-B radiation (Cullen & Lesser 1991; Ekelund 1994). Therefore, the response function is multiplied by an inhibition factor dependent on UV-B radiation:

$$P(I_{PAR}, I_{UVB}) = P_{Max} \cdot \frac{I_{PAR}}{I_{OPT}} \exp\left(-\frac{I_{PAR}}{I_{OPT}} + 1\right) \times \frac{1}{1 + \left(\frac{I_{UVB}}{K_{tr}}\right)^m} \quad (5)$$

where K_{tr} is the UV-B threshold for inhibition of photosynthesis. Figure 12 shows the response curves generated by Eqn 5 for different UV-B levels.

Dispersal and production of the CDOM are modelled by the equation

$$\frac{\partial C_{DOM}}{\partial t} = \frac{\partial}{\partial z}\left[D_{CDOM}\,\frac{\partial}{\partial z} C_{DOM} - C_{DOM} \cdot v_g\right] + \gamma B. \quad (6)$$

The radiation transport for PAR and UV-B is described by the following two equations:

$$\frac{1}{c}\frac{\partial I_{PAR}}{\partial t} + \frac{\partial}{\partial z} I_{PAR} = -\kappa_{PAR}\, I_{PAR}, \quad (7)$$

$$\frac{1}{c}\frac{\partial I_{UVB}}{\partial t} + \frac{\partial}{\partial z} I_{UVB} = -\sigma_{UVB}\, I_{UVB}. \quad (8)$$

Here c is the velocity of light. As our model is a one-dimensional model the zenith dependence of irradiation is modelled by time-varying boundary conditions at the upper boundary. The two attenuation coefficients κ_{PAR} and σ_{UVB} are the sums of a constant term and a term proportional to the algal biomass and the CDOM concentration, respectively:

$$\kappa_{PAR} = \kappa_B + \kappa_p\, B(z, t), \quad (9)$$

$$\sigma_{UVB} = \sigma_B + \sigma_p\, C_{DOM}(z, t). \quad (10)$$

The background attenuation coefficients due to water suspended particles for PAR and UV-B are denoted by K_B and σ_B, respectively. The second terms on the right-hand sides of Eqns (9) and (10) describe the attenuation for PAR due to algal biomass and UV-B due to CDOM. It should be noted that these latter equations yield the Lambert–Beer attenuation equation if the attenuation coefficients are constant.

The above-described model, although of reduced complexity, already allows us to study the importance of CDOM production and negative phototaxis and is thus suited to study the effects of UV-B changes during a polarity transition. Model parameters with standard values are used (see Table 1).

https://doi.org/10.1017/S1473550409990073 Published online by Cambridge University Press

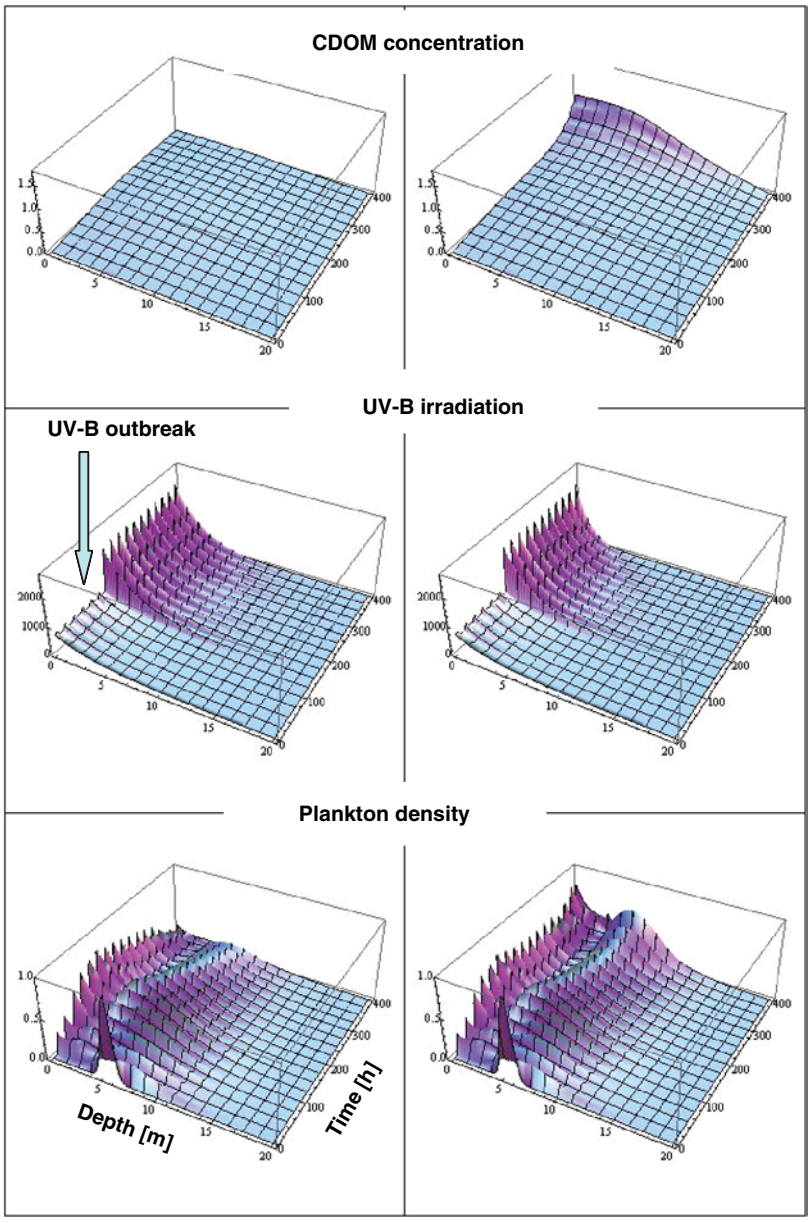

Fig. 14. The effect of UV-B radiation on bio-optical environment and plankton density for different rates of CDOM production. Left column: CDOM production is low. Right column: CDOM production is triggered by a UV-B event.

Figure 13 displays the reaction of the phytoplankton population to daily variations of PAR by phototaxis. The population migrates into the surface layers during the night to reach optimal PAR intensity. During the daytime the population migrates downward, thereby optimizing the rate of photosynthesis.

Figure 14 shows the effect of enhanced UV-B on the bio-optical environment and the plankton population dynamics for two different populations, one with low CDOM production and one with UV-B triggered CDOM production. Protection strategies against UV-B irradiation involve the release of CDOM and negative phototaxis as expressed by the form of the light response curve and the active movement towards a zone of optimal light conditions. For the population with low CDOM production the plankton density varies in the daytime as in Figure 13 before the outbreak of UV-B radiation (Fig. 14, left column). After the breakout the plankton density diminishes in the following hours, eventually causing the death of the whole population.

For a population with CDOM production triggered by enhanced UV-B (see a discussion of this effect by e.g. Morrison & Nelson (2004)) the response to the UV-B outbreak is different. The CDOM concentration increases (Fig. 14, upper right panel), causing increased absorption of UV-B radiation in the water column, and thereby allowing a recovery of the plankton density after the initial decay just after the outbreak. The response to any outbreak depends very much on the CDOM production properties of

https://doi.org/10.1017/S1473550409990073 Published online by Cambridge University Press

the plankton species concerned. Phytoplankton populations certainly have the possibility to survive UV-B outbreaks as expected during polarity transitions and can develop suitable protection mechanisms.

These first simulations already demonstrate how complex the interaction between UV-B radiation and the biosphere can be. No simple linear response should be expected, but parameter-dependent nonlinear and time-delayed responses as well as hysteresis effects are to be expected. Also, in this first model we have omitted the nutritional chain and any long-term genetic effects. These are the subject of ongoing studies.

4 Summary and conclusions

A polarity transition of the geomagnetic field is a major dynamic change of the terrestrial outer fluid core and has been speculated to represent a catastrophic event to the biosphere. A potential connection between the Earth's magnetic field, climate and biosphere was discussed as early as Uffen (1963) and in more recent studies by e.g. Svensmark (2007), Courtillot *et al*. (2007) and Knudsen & Riisager (2009). In these studies the galactic cosmic ray (GCR) theory has been advocated suggesting a link between geomagnetic field modulations of the GCR flux and climate variations. As the GCR flux is also modulated by the solar wind magnetic field the GCR theory presents a very interesting hypothesis for a better understanding of the Sun–Earth connection.

Another possible mechanism coupling solar activity, geomagnetic field variations and terrestrial ecosystems is via the production of NO_X in the middle atmosphere caused by SPEs during geomagnetic polarity transitions. Recent studies on this topic have been reviewed and allow us to draw the following conclusions.

- During a polarity transition the size of the terrestrial magnetosphere is significantly smaller than its current size, but never vanishes. It always exists and is the prime terrestrial shield against the hot solar wind plasma.
- The paleomagnetosphere is topologically much more complex and is intrinsically more dynamic than the current magnetosphere.
- Due to the significantly weaker geomagnetic field, solar energetic protons have much better access to the middle atmosphere. Their impact area is almost 100%.
- During polarity transitions SPEs cause significant NO_X production, preferentially transported downward to the stratosphere in polar regions.
- A major atmospheric effect of polarity transitions is most probably the generation of a natural ozone hole due to enhanced SPE activity. This ozone hole is associated with a strong increase of erythemal weighted surface UV-B flux.
- The increase of erythemal weighted surface UV-B flux represents a clear stress on aquatic ecosystems such as phytoplankton populations. Using a simplified model of enhanced UV-B stress on such a population indicates a complex, nonlinear response of the population.
- The chain of processes from solar activity to effects on the Earth system is a rather complex one. This makes correlative studies between the discussed Sun–Earth connection rather difficult.
- Future studies should, for example, investigate biologic indicators from geological archives from marine and lacustrine ecosystems. A suitable parameter would be a proxy of CDOM density in sediment layers as CDOM can be used as an indicator of increased UV-B level.

We conclude that many further studies on details of the suggested process chain and actual analyses of geologic proxies are necessary before a possible connection following the processes discussed can be confirmed. All recent studies do not yet allow one to decide whether a polarity transition is a cataclysm to the Earth system or not.

Acknowledgement

The work of KHG and JV was financially supported by the Deutsche Forschungsgemeinschaft.

References

Baumgartner, S., Beer, J., Masarik, J., Wagner, G., Meynadier, L. & Synal, H.-A. (1998). Geomagnetic modulation of the 36Cl flux in the GRIP ice core Greenland. *Science* **279**, 1330–1334. doi: 10.1126/science.279.5355.1330.

Black, D.I. (1967). Cosmic ray effects and faunal extinctions at geomagnetic field reversals. *Earth Planet. Sci. Lett.* **3**, 225–236. doi: 10.1016/0012-821X(67)90042-8.

Casale, G.R., Meloni, D., Miano, S., Palmieri, S., Siani, A.M. & Cappellani, F. (2000). Solar UV-B irradiance and total ozone in Italy: fluctuations and trends. *J. Geophys. Res.* **105**, 4895–4902. doi: 10.1029/1999JD900303.

Chattopadhyay, J. & Sarkar, R.R. (2003). Chaos to order: preliminary experiments with a population dynamics model of three trophic levels. *Ecol. Mod.* **163**, 45–50.

Cockell, C.S. & Blaustein, A.R.(eds). (2001). *Ecosystems, Evolution, and Ultraviolet Radiation*. Springer, Berlin.

Constable, C.G. & Parker, R.L. (1988). Statistics of the geomagnetic secular variation for the past 5 m.y. *J. Geophys. Res.* **93**, 11 569–11 578. doi: 10.1029/JB093iB10p11569.

Courtillot, V., Gallet, Y., Le Mouël, J.-L., Fluteau, F. & Genevey, A. (2007). Are there connections between the Earth's magnetic field and climate? *Earth Planet. Sci. Lett.* **253**, 328–339.

Crutzen, P.J., Isaksen, I.S.A. & Reid, G.C. (1975). Solar Proton Events: stratospheric sources of nitric oxide. *Science* **189**, 457–459. doi: 10.1126/science.189.4201.457.

Cullen, J.J. & Lesser, P.M. (1991). Photoinhibition by uv-b radiation. *Marine Biology* **111**, 183–190.

Eilers, P.H.C. & Peeters, J.C.H. (1988). A model for the relationship between light intensity and the rate of photosynthesis in phytoplankton. *Ecol. Model.* **42**, 199–215.

Ekelund, N. (1994). Influence of UV-b radiation on photosynthetic light response curves, absorption spectra and motility of four phytoplankton species. *Physiologica Plantarum* **91**, 696–702.

Fabian, K. & Leonhardt, R. (2009). Records of paleomagnetic field variations. In *Geomagnetic Variations*, eds Glassmeier, K.H., Soffel, H. & Negendank, J.W., pp. 65–106. Springer, Berlin.

Glassmeier, K., Vogt, J., Stadelmann, A. & Buchert, S. (2004). Concerning long-term geomagnetic variations and space climatology. *Ann. Geophys.* **22**, 3669–3677.

Glassmeier, K.H., Soffel, H. & Negendank, J.W. (eds). (2009). *Geomagnetic Variations*. Springer, Berlin.

Glatzmaier, G.A. & Roberts, P.H. (1995). A three-dimensional self-consistent computer simulation of a geomagnetic field reversal. *Nature* **377**, 203–207. doi: 10.1038/377203a0.

Gröbner, J. *et al*. (2000). Variability of spectral solar ultraviolet irradiance in an alpine environment. *J. Geophys. Res.* **105**, 26 991–27 004. doi: 10.1029/2000JD900395.

Guyodo, Y. & Valet, J.-P. (1999). Global changes in intensity of the Earth's magnetic field during the past 800kyr. *Nature* **399**, 249–252. doi: 10.1038/20420.

Häder, D.-P. (2001). Ultraviolet radiation and aquatic microbial ecosystems. In *Ecosystems, Evolution, and Ultraviolet Radiation*, eds Cockell, C.C. & Blaustein, A.R., pp. 150–169. Springer, Berlin.

Häder, D.-P., Kumar, H.D., Smith, R.C. & Worrest, R.C. (2007). Effects of solar uv radiation on aquatic ecosystems and interaction with climate change. *Photochem. Photobiol. Sci.* **6**, 267–285.

Hays, J.D. (1971). Faunal extinctions and reversals of the Earth's magnetic field. *Geol. Soc. Am. Bull.* **82**, 2433–2447.

Hays, J.D. (1972). Faunal extinctions and reversals of the earth's magnetic field: Reply. *Geol. Soc. Am. Bull.* **83**, 2215.

Jackman, C.H., McPeters, R.D., Labow, G.J., Fleming, E.L., Praderas, C.J. & Russell, J.M. (2001). Northern hemisphere atmospheric effects due to the July 2000 solar proton event. *Geophys. Res. Lett.* **28**, 2883–2886. doi: 10.1029/2001GL013221.

Kallenrode, M.-B. (2004). *Space Physics: An Introduction to Plasmas, and Particles in the Heliosphere and Magnetospheres*. Springer, Berlin.

Klausmeier, C.A. & Lichman, E. (2001). Algal games: the vertical distribution of phytoplankton in poorly mixed water columns. *Limnol. Oceanogr.* **46**, 1998–2007.

Knudsen, M.F. & Riisager, P. (2009). Is there a link between Earth's magnetic field and low-latitude precipiation? *Geology* **37**, 71–74.

Korte, M. & Constable, C.G. (2006). Centennial to millennial geomagnetic secular variation. *Geophys. J. Int.* **167**, 43–52. doi: 10.1111/j.1365-246X.2006.03088.x.

Kuwahara, V.S., Ogawa, H., Toda, T., Kikuchi, T. & Taguchi, S. (2000). Variability of bio-optical factors influencing the seasonal attenuation of ultraviolet radiation in temperate coastal waters of japan. *Photochem. Photobiol.* **72**, 193–199.

Leonhardt, R. & Fabian, K. (2007). Paleomagnetic reconstruction of the global geomagnetic field evolution during the Matuyama/Brunhes transition: Iterative Bayesian inversion and independent verification. *Earth Planet. Sci. Lett.* **253**, 172–195. doi: 10.1016/j.epsl.2006.10.025.

Madronich, S., McKenzie, R.L., Björn, L.O. & Caldwell, M.M. (1998). Changes in biologically active ultraviolet radiation reaching the earth's surface. *UNEP Environmental Effects Panel Report*, pp. 5–19. United Nations, New York.

Mann, C.J. (1972). Faunal extinctions and reversals of the earth's magnetic field: Discussion. *Geol. Soc. Am. Bull.* **83**, 2211–2214.

Marshall, H. (1928). Ultra-violet and extinction. *The American Naturalist* **62**, 165–187.

McHargue, L.R., Donahue, D., Damon, P.E., Sonett, C.P., Biddulph, D. & Burr, G. (2000). Geomagnetic modulation of the late Pleistocene cosmic-ray flux as determined by 10Be from Blake Outer Ridge marine sediments. *Nucl. Instrum. Methods Phys. Res. B* **172**, 555–561. doi: 10.1016/S0168-583X(00)00092-6.

Merrill, R.T. & McFadden, P.L. (1999). Geomagnetic polarity transitions. *Rev. Geophys.* **37**, 201–226.

Mewaldt, R.A. (2006). Solar energetic particle composition, energy spectra, and space weather. *Space Sci. Rev.* **124**, 303–316. doi: 10.1007/s11214-006-9091-0.

Morrison, J.R. & Nelson, B.N. (2004). Seasonal cycle of phytoplankton uv absorption at the bermuda atlantic time-series site. *Limnol. Oceanogr.* **49**, 215–224.

Plotnick, R.E. (1980). Relationship between biological extinctions and geomagnetic reversals. *Geology* **8**, 578–581.

Raup, D.M. (1985). Magnetic reversals and mass extinctions. *Nature* **314**, 341–343. doi: 10.1038/314341a0.

Reid, G.C., Solomon, S. & Garcia, R.R. (1991). Response of the middle atmosphere to the solar proton events of august-december, 1989. *Geophys. Res. Lett.* **18**, 1019–1022. doi: 10.1029/91GL01049.

Selkin, P. & Tauxe, L. (2000). Long term variations in geomagnetic field intensity. *Phil. Trans. Roy. Soc.* **358**, 869–1223.

Sinnhuber, M., Burrows, J.P., Chipperfield, M.P., Jackman, C.H., Kallenrode, M.-B., Künzi, K.F. & Quack, M. (2003). A model study of the impact of magnetic field structure on atmospheric composition during solar proton events. *Geophys. Res. Lett.* **30**, ASC 10-1. doi: 10.1029/2003GL017265.

Siscoe, G.L. & Chen, C.-K. (1975). The paleomagnetosphere. *J. Geophys. Res.* **80**, 4675–4680. doi: 10.1029/JA080i034p04675.

Siscoe, G.L. & Crooker, N.J. (1976). Auroral zones in a quadrupole magnetosphere. *J. Geomagn. Geoelectr.* **28**, 1–9.

Smart, D.F., Shea, M.A. & Flückiger, E.O. (2000). Magnetospheric models and trajectory computations. *Space Sci. Rev.* **93**, 305–333.

Soffel, H. (1991). *Paläomagnetismus und Archäomagnetismus*. Springer, Heidelberg, 1991.

Solomon, S. (1988). The mystery of the Antarctic ozone 'hole'. *Rev. Geophys.* **26**, 131–148. doi: 10.1029/RG026i001p00131.

Stadelmann, A. (2004). Globale Effekte einer Magnetfeldumkehr: Magnetosphärenstruktur und kosmische Teilchen. *Dissertation*, Technische Universität Braunschweig.

Stadelmann, A., Vogt, J., Glassmeier, K.H., Kallenrode, M.-B. & Voigt, G.H. (2009). Cosmic ray and solar energetic particle flux in paleomagnetospheres. *Earth, Planets, Space* **61**, in press.

Staehelin, J., Harris, N.R.P., Appenzeller, C. & Eberhard, J. (2001). Ozone trends: a review. *Rev. Geophys.* **39**, 231–290. doi: 10.1029/1999RG000059.

Steele, J.H. (1962). Environmental control of photosynthesis in the sea. *Limnol. Oceanogr.* **7**, 137–150.

Steinberg, S., Nelson, N., Carlson, C. & Prusk, A. (2004). Production of chromophoric dissolved organic matter (cdom) in the open ocean by zooplankton and the colonial cyanobacterium trichodesmium spp. *Mar. Ecol. Prog. Ser.* **2647**, 47.

Svensmark, H. (2007). Cosmoclimatology: a new theory emerges. *Astronomy & Geophysics* **48**, 1.18–1.24.

Svensmark, H., Pedersen, J.O.P., Marsh, N.D., Enghoff, M.B. & Uggerhøj, U.I. (2007). Experimental evidence for the role of ions in particle nucleation under atmospheric conditions. *Proc. Royal Soc. London, Series A* **463**, 385–396. doi: 10.1098/rspa.2006.1773.

Tarduno, J.A., Cottrell, R.D., Watkeys, M.K. & Bauch, D. (2007). Geomagnetic field strength 3.2 billion years ago recorded by single silicate crystals. *Nature* **446**, 657–660.

Tinsley, B.A. & Deen, G.W. (1991). Apparent tropospheric response to MeV–GeV particle flux variations: A connection via electrofreezing of supercooled water in high-level clouds? *J. Geophys. Res.* **96**, 22 283–22 296. doi: 10.1029/91JD02473.

Uffen, R.J. (1963). Influence of the Earth's Core on the origin and evolution of life. *Nature* **198**, 143–144. doi: 10.1038/198143b0.

Vogt, J. & Glassmeier, K.-H. (2000). On the location of trapped particle populations in quadrupole magnetospheres. *J. Geophys. Res.* **105**, 13 063–13 072. doi: 10.1029/2000JA900006.

Vogt, J., Zieger, B., Stadelmann, A., Glassmeier, K.-H., Gombosi, T.I., Hansen, K.C. & Ridley, A.J. (2004). MHD simulations of quadrupolar paleomagnetospheres. *J. Geophys. Res.* **109**, A12221. doi: 10.1029/2003JA010273.

Vogt, J., Zieger, B., Glassmeier, K.-H., Stadelmann, A., Kallenrode, M.-B., Sinnhuber, M. & Winkler, H. (2007). Energetic particles in the paleomagnetosphere: Reduced dipole configurations and quadrupolar contributions. *J. Geophys. Res.* **112**, A06216. doi: 10.1029/2006JA012224.

Vogt, J., Sinnhuber, M. & Kallenrode, M.-B. (2009). Effects of geomagnetic variations on system Earth. In *Geomagnetic Variations*, ed. Glassmeier, K.H., Soffel, H. & Negendank, J.W., pp. 159–208. Springer, Berlin.

Voigt, G.-H. (1981). A mathematical magnetospheric field model with independent physical parameters. *Planet. Space Sci.* **29**, 1–20. doi: 10.1016/0032-0633(81)90134-3.

Watkins, N.D. & Goodell, H.G. (1967). Geomagnetic polarity change and faunal extinction in the southern ocean. *Science* **156**, 1083–1087.

Winkler, H., Sinnhuber, M., Notholt, J., Kallenrode, M.-B., Steinhilber, F., Vogt, J., Zieger, B., Glassmeier, K.-H. & Stadelmann, A. (2008). Modeling impacts of geomagnetic field variations on middle atmospheric ozone responses to solar proton events on long timescales. *J. Geophys. Res.* **113**, 2302–2316. doi: 10.1029/2007JD008574.

Zieger, B., Vogt, J., Glassmeier, K.-H. & Gombosi, T.I. (2004). Magnetohydrodynamic simulation of an equatorial dipolar paleomagnetosphere. *J. Geophys. Res.* **109**, A7205. doi: 10.1029/2004JA010434.

Zieger, B., Vogt, J. & Glassmeier, K.-H. (2006). Scaling relations in the paleomagnetosphere derived from MHD simulations. *J. Geophys. Res.* **111**, A6203. doi: 10.1029/2005JA011531.